Preparation of magnetic core mesoporous shell microspheres with C18-modified interior pore-walls for fast extraction and analysis of phthalates in water samples

Zhongbo Li[a], Danni Huang[a], Chinfai Fu[a], Biwen Wei[b], Wenjia Yu[b], Chunhui Deng[a,*], Xiangmin Zhang[a]

[a] Department of Chemistry, Fudan University, No. 220, Handan Road, Shanghai 200433, China
[b] Shanghai Entry-Exit Inspection and Quarantine Bureau, Shanghai 200135, China

ARTICLE INFO

ABSTRACT

In this study, core–shell magnetic mesoporous microspheres with C18-functionalized interior pore-walls were synthesized through coating Fe_3O_4 microspheres with a mesoporous inorganic–organic hybrid layer with a n-octadecyltriethoxysilane (C18TES) and tetraethyl orthosilicate (TEOS) as the silica source and cetyltrimethylammonia bromide (CTAB) as a template. The obtained C18-functionalized $Fe_3O_4@mSiO_2$ microspheres possess numerous C18 groups anchored in the interior pore-walls, large surface area (274.7 m^2/g), high magnetization (40.8 emu/g) and superparamagnetism, uniform mesopores (4.1 nm), which makes them ideal absorbents for simple, fast, and efficient extraction and enrichment of hydrophobic organic compounds in water samples. Several kinds of phthalates were used as the model hydrophobic organic compounds to systematically evaluate the performance of the C18-functionalized $Fe_3O_4@mSiO_2$ microspheres in extracting hydrophobic molecules by using a gas chromatography–mass spectrometry. Various parameters, including eluting solvent, the amounts of absorbents, extraction time and elution time were optimized. Hydrophobic extraction was performed in the interior pore of magnetic mesoporous microspheres, and the materials had the anti-interference ability to macromolecular proteins, which was also investigated in the work. Under the optimized conditions, C18-functionalized $Fe_3O_4@mSiO_2$ microspheres were successfully used to analyze the real water samples. The results indicated that this novel method was fast, convenient and efficient for the target compounds and could avoid being interfered by macromolecules.

1. Introduction

Mesoporous silica-based materials, which have been used to adsorb various organic molecules in order to provide new platforms of their functions, have brought an explosive influence in the past decade [1,2]. Because of their attractive features of very high specific surface areas, thermal and mechanical stability, highly uniform pore distribution and tunable pore size, high adsorption capacity and unprecedented hosting properties, as well as extraordinarily wide possibilities of functionalization [3–9], they have won themselves ample host–guest chemistry and integrated functional properties [10]. Recently, organic–inorganic hybrid mesoporous silica materials, which were obtained by anchoring organic moieties to mesoporous silica surface, have attracted great attentions for the application to the extraction of contaminations [11–13]. The introduction of organic groups into an inorganic network or surface leads to new variation of structural properties, thereby promoting new potential applications for the resulting organic–inorganic hybrid materials [14]. Magnetic mesoporous silica, which combines the advantages of mesoporous structure and strong magnetization, is a typical hybrid material, and has attracted great attentions for the use in the extraction of contaminations [15–17]. Synthesis of functionalized magnetic mesoporous silica materials and their application to environmental treatment and analysis have been a research of hot point [18–26]. In our previous work, we had successfully synthesized magnetic mesoporous microspheres for the fast separation of the hydrophilic compound of microcystins in water [27,28]. The as-made mesoporous silica microspheres with sandwich structure were synthesized with a silica-coated magnetite core and ordered mesoporous silica shell using a surfactant-templating approach. More recently, our group developed a very simple approach for directly coating mesoporous silica shell on magnetic microspheres for the extraction and separation of low-concentration hydrophilic microcystin-LR in water [29,30]. The development of functionalized magnetic mesoporous silica for the extraction and analysis of hydrophobic pollutants in environmental samples is very interesting and important. However, to our best knowledge, few related work was reported.

* Corresponding author. Tel.: +86 21 6564 3983; fax: +86 21 6564 1740.
E-mail address: chdeng@fudan.edu.cn (C. Deng).

In this study, for the first time, we successfully synthesized magnetic core–mesoporous shell microspheres with C18-modified interior pore-walls and applied them to the extraction and analysis of hydrophobic organic compounds in water samples. In this work, phthalates were selected as the model hydrophobic compounds to investigate the extraction ability of the as-made materials because they are ubiquitous pollutants in water and can enter the human body directly or indirectly through different pathways, causing malformation and cancer [31–34]. Herein, at first, C18-functionalized magnetic core–mesoporous shell microspheres were synthesized and characterized. And then the as-made materials were applied as the magnetic adsorbent to the extraction and analysis of hydrophobic compounds of phthalates in water by gas chromatography–mass spectrometry (GC–MS).

2. Materials and methods

2.1. Chemicals

The phthalate standards containing dimethyl phthalate (DMP), diethyl phthalate (DEP), di-iso-butyl phthalate (DIBP), di-n-butyl phthalate (DBP), di-(2-ethylhexyl) phthalate (DEHP), benzylbutyl phthalate (BBP) and di-n-octyl phthalate (DNOP) were purchased from Dr. Ehrenstorfer (Augsburg, Germany). $FeCl_3 \cdot 6H_2O$, tetraethyl orthosilicate (TEOS), ethylene glycolethanol and cetyltrimethyl ammonium bromide (CTAB) were purchased from Shanghai Chemical Corp. *n*-Octadecyltriethoxysilane (C18TES, Purity > 95%) was purchased from Alfa Aesar (Tianjin, China). Deionized water was purified by a Milli-Q system (Milford, MA, USA).

The standard solution of phthalates was prepared by diluting the phthalates in acetone with a concentration of 2.0 mg/L. The working standard solution was stored under 4 °C and was found to be stable for 3 months.

2.2. Synthesis of C18–Fe₃O₄@mSiO₂ microspheres

Magnetic Fe_3O_4 microspheres with a mean diameter of 250 nm were synthesized according to previously reported method [35]. The C18-functionalized $Fe_3O_4@mSiO_2$ microspheres were synthesized through a surfactant involved sol–gel process according to previous method with some modifications [27,36,37]. The as-prepared Fe_3O_4 microspheres and CTAB with a ratio of 50 mg/500 mg were dispersed in 50 mL of deionized water and sonicated for 30 min. The resultant dispersion was mixed with 450 mL of NaOH aqueous solution and further sonicated for 5 min to form a stable dispersion. The resultant dispersion was then heated at 60 °C for 30 min. Afterwards, 2.5 mL of tetraethylorthosilicate (TEOS)/ethanol (v/v: 1/4) solution was added drop by drop under mechanical stirring, followed by heating at 60 °C for 30 min with stirring. Subsequently, 150 μL of TEOS/*n*-octadecyltriethoxysilane (C18TES) (v/v: 2:1) mixed solution was injected into the dispersion, and this dispersion was further heated at 60 °C for 12 h. The product was collected by magnetic separation and refluxed in ethanol at 60 °C to remove the CTAB templates thoroughly. Finally, the resulting C18-functionalized $Fe_3O_4@mSiO_2$ microspheres were dried at 50 °C for 24 h in vacuum for future use.

2.3. Measurements and characterizations

The morphology of C18-functionalized $Fe_3O_4@mSiO_2$ microspheres was investigated using transmission electron microscopy (TEM) (JEOL 2011 microscope, Japan) and scanning electron microscopy (SEM) (Philips XL30 electron microscope, Netherlands). The surface modification of C18-functionalized $Fe_3O_4@mSiO_2$ microspheres was investigated by Fourier-transform infrared

(FTIR) spectroscopy (Nicolet Nexus 470). Nitrogen sorption isotherms were measured at 77 K with a Micrometrics Tristar 3000 analyzer (USA). The retention of BSA on the C18-functionalized $Fe_3O_4@mSiO_2$ microspheres was studied by ultraviolet–visible spectrophotometer (Agilent 8453).

2.4. The micro solid-phase extraction (MSPM) procedure by C18-functionalized Fe₃O₄@mSiO₂ microspheres

A water sample from Yangpu River was used for this study. First, 10 mL of water sample containing phthalates with a concentration of 100 ng/mL was added in a 10 mL vial with PTFE-silicone septum. Then 10 mg of C18-functionalized $Fe_3O_4@mSiO_2$ microspheres were added in the vial to extract the analytes, and the mixture was vibrated equably to make the particles contact entirely with water sample. After 15 min, a magnet bar was placed beside the vial to hold the C18-functionalized $Fe_3O_4@mSiO_2$ microspheres which had already extracted the analytes. Subsequently the water was removed from the vial with the sorbent remained in the vial. The analytes were eluted by 500 μL chloroform under ultrasonic condition. Finally, 1 μL of eluting solution was injected into GC–MS to analyze.

2.5. The investigation of anti-interference ability

As we know, proteins, which are from rotten animal skins, fairs, metabolites, etc., universally exist in real water samples. In order to determine the anti-interference ability of the adsorbent to macromolecular proteins, BSA was selected as the model protein. Here, 200 μg of BSA was added into 10 mL of water sample which contained 100 μg/L trace target contaminations. And then the mixture was extracted by 10 mg of C18-functionalized $Fe_3O_4@mSiO_2$ microspheres and eluted with 500 μL of chloroform; subsequently the elution was determined by GC–MS.

2.6. Instrument and chromatographic conditions

GC–MS instrument (6890GC/5973, Agilent Co.) was used to the determination of phthalates. The extracted compounds were separated on an HP-5MS capillary column (30 m × 0.25 mm, 0.25 μm), and the sample was injected in splitless mode. The column oven temperature was programmed with an initial temperature of 60 °C for 1 min, raised to 280 °C with a ramping rate of 15 °C/min, and then hold for 4 min. The injection temperature was 250 °C. Helium (99.999%) was used as the carrier gas with a flow rate of 1 mL/min. All samples were analyzed in selected ion monitoring (SIM) mode.

2.7. Analytical validations

The five-point calibration curve of the each phthalate was fabricated by plotting peak areas (y) of phthalate versus corresponding concentration of the analyte (x). Concentrations of phthalates in water sample were calculated from each resulting peak area ratios and each regression equation of the calibration curve.

Five replicate injections of same standard samples of phthalates were analyzed by the GC–MS method to determine reproducibility in the conditions (system precision). The limit of detection (LOD) (S/N = 3) of the method was calculated by the analysis of the standard solution with low concentration. And the limit of quantification (LOQ) was calculated on the basis of S/N = 10. In addition, the recoveries of the target compounds were studied by extracting the spiked water sample (1 μg/mL) under the optimized conditions for three times.
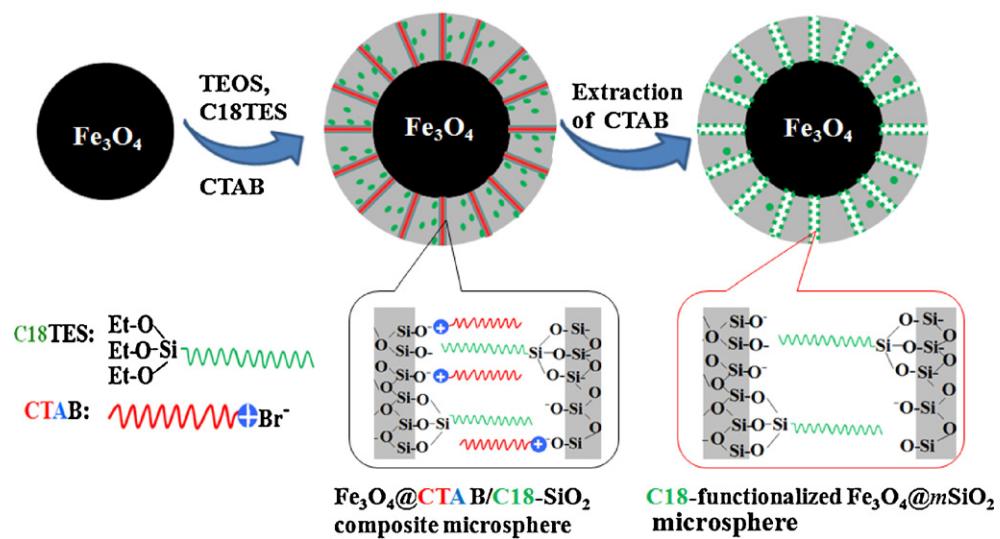
Scheme 1. The synthetic procedure of core–shell structured C18-functionalized $Fe_3O_4@mSiO_2$ microspheres.
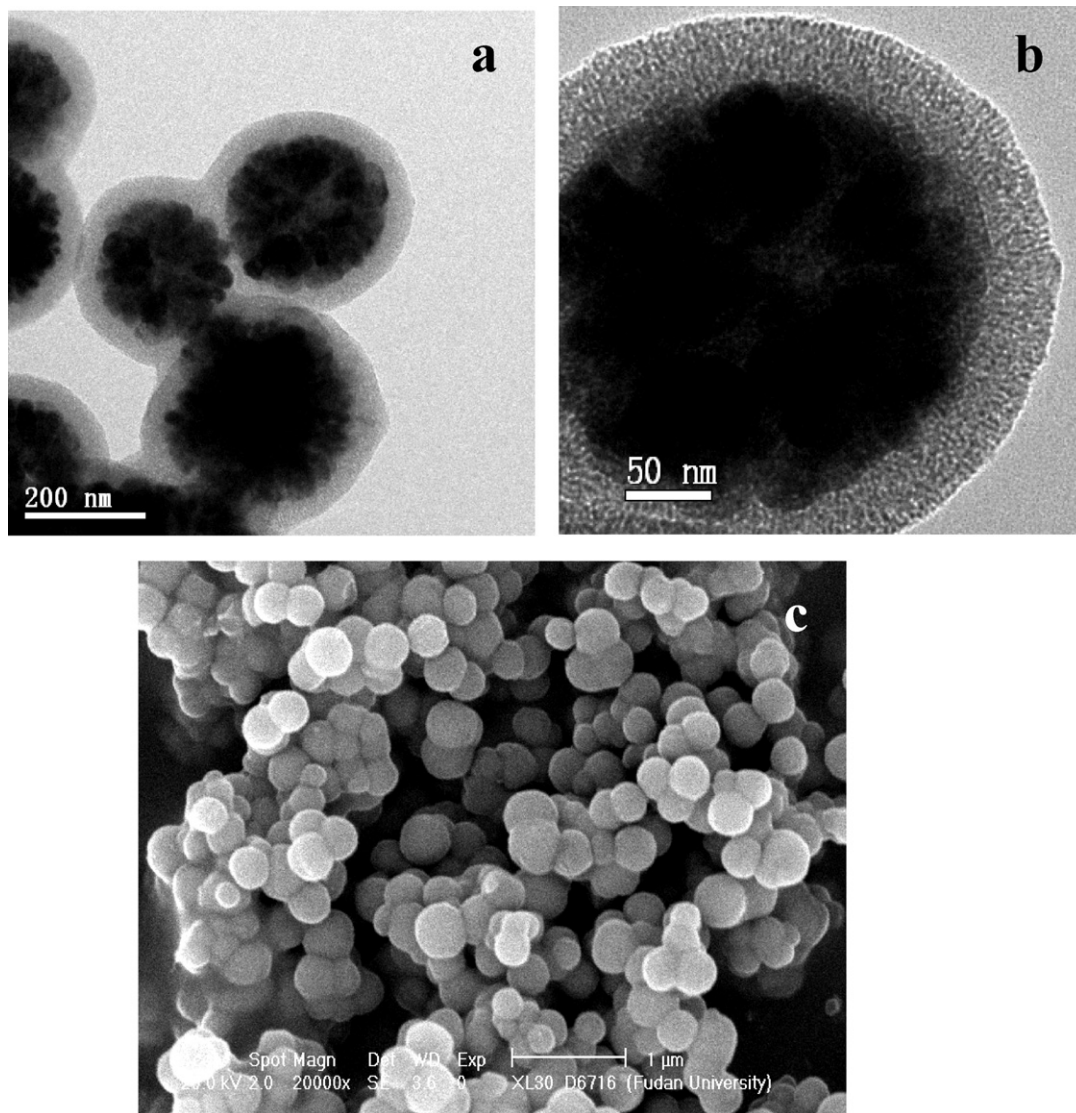

Fig. 1. (a and b) TEM images and (c) SEM images of the synthesized C18-functionalized $Fe_3O_4@mSiO_2$ microspheres.

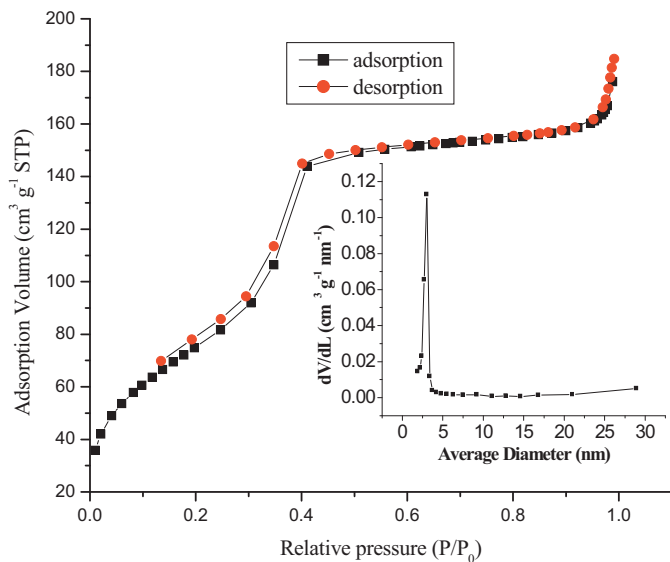**Fig. 2.** Nitrogen adsorption–desorption isotherms and pore size distribution (inset) of the C18-functionalized $Fe_3O_4@mSiO_2$ microspheres recorded at 77 K.

3. Results and discussion

3.1. Synthesis and characterization of the C18–$Fe_3O_4@mSiO_2$ microspheres

The procedure for synthesis of C18-functionalized $Fe_3O_4@mSiO_2$ microspheres is illustrated in Scheme 1. By using the facile one-pot synthesis approach, C18-functionalized $Fe_3O_4@mSiO_2$ microspheres were synthesized through the co-condensation of TEOS and n-octadecyltriethoxysilane (C18TES) in the presence of Fe_3O_4 microspheres as the seeds and CTAB as the template [37,38]. SEM image shows that the obtained microspheres have a narrow size distribution and an average diameter of 300 nm (Fig. 1c). TEM image indicates a dark magnetic core with diameter of about 250 nm and a gray porous silica shell with thickness of about 50 nm (Fig. 1a). Large-magnification TEM image (Fig. 1b) indicates that the pore channels in the shell are perpendicular to the microsphere's surface, which is similar to previous reports [27,39–41].

The porosity of the C18-functionalized $Fe_3O_4@mSiO_2$ microspheres was studied by N_2 adsorption–desorption measurement at 77 K. The N_2 adsorption–desorption isotherms show representative type IV curves with a sharp capillary condensation step at a relative pressure of 0.2–0.4, indicative of a small cylindrical pore. The pore size distribution derived from the adsorption branch using the Barrett–Joyner–Halenda (BJH) method indicates that the obtained materials have a pore size of about 4.1 nm with a narrow pore size distribution (Fig. 2, inset). The BET surface area and total pore volume were calculated to be 274.7 m^2/g and 0.28 cm^3/g, respectively, indicating a high porosity.

To confirm the presence of C18-groups in the C18-functionalized $Fe_3O_4@mSiO_2$ microspheres obtained by the co-condensation coating process, magnetic mesoporous silica ($Fe_3O_4@mSiO_2$) microspheres were synthesized through the same method without using C18TES. Fourier-transform infrared (FT-IR) spectra of C18-functionalized $Fe_3O_4@mSiO_2$ microspheres (Fig. 3a) and $Fe_3O_4@mSiO_2$ (Fig. 3b) microspheres were recorded. In Fig. 3a, the peaks at 575 and 1078 cm^{-1} are attributed to the characteristic absorption of Fe–O–Fe and Si–O–Si vibrations, respectively. The broad bands at 3411, 1556 and 960 cm^{-1} are from O–H stretching and Si–OH stretching. In the FT-IR spectrum of C18-functionalized $Fe_3O_4@mSiO_2$ (Fig. 3a), the new
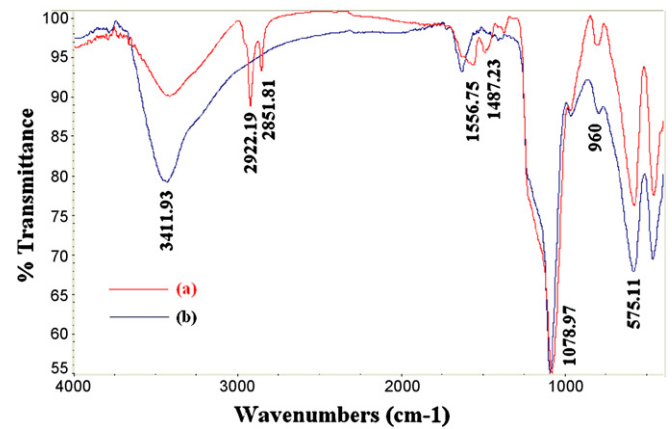

Fig. 3. The FT-IR spectra of (a) C18-functionalized $Fe_3O_4@mSiO_2$ microspheres and (b) $Fe_3O_4@mSiO_2$ microspheres.

absorption peak at 2922 cm^{-1} is attributed to C–H vibration of –CH_3, and 2851 cm^{-1} and 1487 cm^{-1} were from C–H vibration of –CH_2, indicating that the C18 alkyl groups are present in the C18-functionalize $Fe_3O_4@mSiO_2$ microspheres. Similar to the $Fe_3O_4@mSiO_2$ microspheres, the C18-functionalized magnetic mesoporous silica microspheres obtained through the one-pot synthesis display an excellent dispersibility in aqueous solution (Fig. 4a), reflecting numerous silanol groups on the exterior surface of the microspheres. However, further functionalization of the $Fe_3O_4@mSiO_2$ microspheres by post grafting of C18TES can generate C18-grafted $Fe_3O_4@mSiO_2$ microspheres which show poor dispersibility in water (Fig. 4b). The poor aqueous dispersibility is due to the fact that both the interior and the exterior surfaces of the mesoporous microspheres can be modified by hydrophobic C18 groups. The results mentioned above verified that a considerable amount of C18 groups are presence in the interior pore wall.

The magnetic properties of C18-functionalzied $Fe_3O_4@mSiO_2$ microspheres were investigated on a superconductive quantum interference device (SQUID) at room temperature. Fig. 5
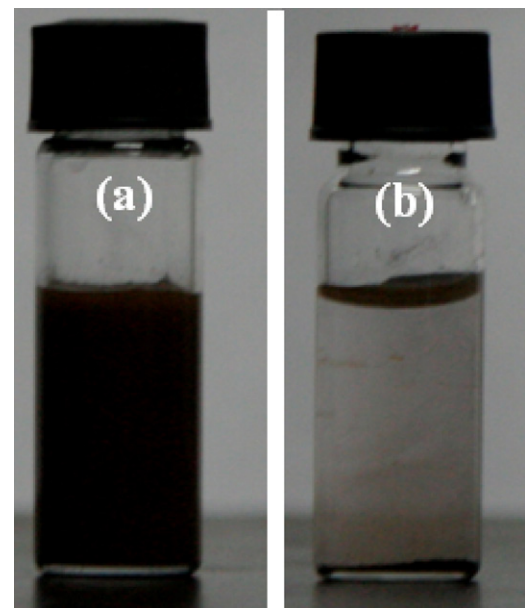

Fig. 4. Optical photographs of aqueous dispersions of (a) C18-functionlaized $Fe_3O_4@mSiO_2$ microspheres synthesized through the one-pot method and (b) C18-grafted $Fe_3O_4@mSiO_2$ through two-step method by grafting C18 onto the $Fe_3O_4@mSiO_2$ microspheres.
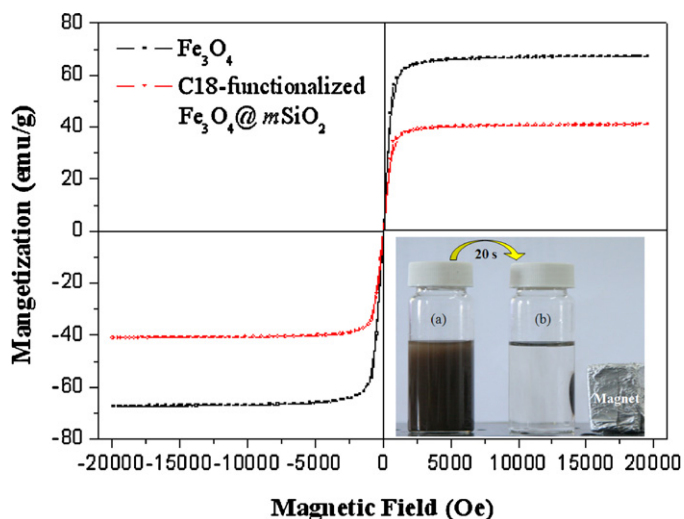
Fig. 5. Magnetization curves of Fe_3O_4 and C18-functionalized $Fe_3O_4@mSiO_2$ and the. separation and redispersion process (inset) of the C18–$Fe_3O_4@mSiO_2$.

Fig. 6. The optimization of eluting solvent (chloroform, ethyl acetate and acetone). Error bar represents disperse of 3 runs.

shows magnetization curves of Fe_3O_4 and C18-functionalized $Fe_3O_4@mSiO_2$ microspheres, the magnetic materials exhibit a superparamagnetic behavior, that is, no remanence was detected at room temperature. Maximum saturation magnetization (40.8 emu/g) of C18-functionalized $Fe_3O_4@mSiO_2$ is a little less than that (67.2 emu/g) of Fe_3O_4 microspheres due to the nonmagnetic mesoporous silica shell and C18 groups. According to Ma's study, this saturation magnetization can ensure a fast magnetic separation process with a magnet in practical application [42]. All the above results showed that the C18-functionalized magnetic mesoporous microspheres with high magnetic responsivity were successfully synthesized using the proposed approach.

3.2. Optimization of extraction conditions

Because C18-functionalized $Fe_3O_4@mSiO_2$ microspheres have the hydrophobic C18 groups in the inner pore-walls, they can be used to extract and enrich hydrophobic analytes by the hydrophobic–hydrophobic interaction. To investigate the enrichment efficiency of the C18-functionalized $Fe_3O_4@mSiO_2$ microspheres, phthalates in water were applied as the model hydrophobic organic compounds. Also extraction conditions were optimized in the following work.

The selection of the kinds of eluting solvent is quite important for the extraction of analytes by C18-functionalized $Fe_3O_4@mSiO_2$ microspheres. In the extraction process, it is important to maximize the analytes concentration, so the selection of a proper solvent to elute the analytes is quite necessary. In this study, we selected acetone, ethyl acetate and chloroform to be studied, and then compared their eluting efficiencies. The results were shown in Fig. 6. As seen from Fig. 6, chloroform had the highest efficiency, while acetone had a relative low adsorbing efficiency. It could be explained as that chloroform has the similar polarity with phthalates which are the analytes, so the solvent of chloroform could elute phthalic esters more easily than ethyl acetate and acetone. Therefore, chloroform was selected as the optimized eluting solvent in the following work.

The volume of elution solvent is also an important factor to obtain reliable and reproducible analytical results. In this work, to investigate the influence to the extraction recovery, 300, 500 and 800 μL chloroform were selected. Fig. 7 shows that the maximum extraction efficiency of these analytes was obtained when the elution volume reached to 500 μL.
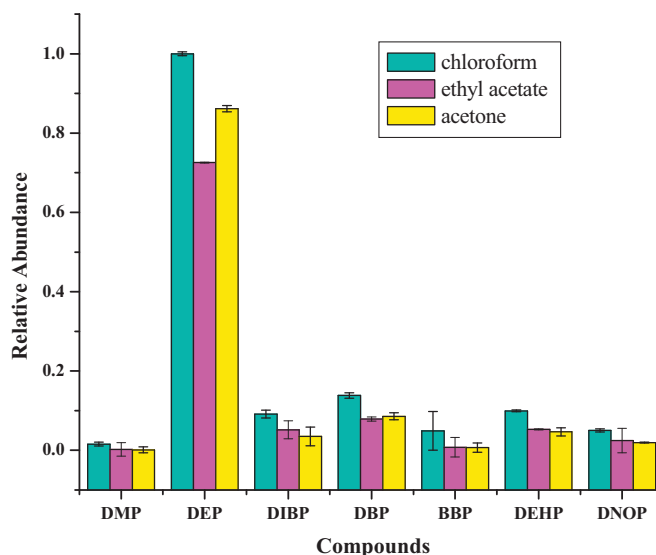
To obtain the maximum extraction efficiency of target analytes, the amounts of the adsorbents required was optimized by varying C18-functionalized $Fe_3O_4@mSiO_2$ microspheres amount from 3 to 50 mg. As the result shown in Fig. 8, only 10 mg of the C18–$Fe_3O_4@mSiO_2$ sorbents was enough to attain satisfactory results because of the large surface area and high adsorption efficiency of the mesoporous nanosorbent. So, the optimal amount of C18-functionalized $Fe_3O_4@mSiO_2$ microspheres was 10 mg.

In order to enhance extraction efficiency, a certain standing time is required after the sorbents are dispersed into the solution. In this research, different extraction time (5, 10, 15 and 30 min) was studied. As shown in Fig. 9, the extraction efficiencies of all phthalates were enhanced with an increasing time, and the maximum extraction efficiency of these analytes was obtained when the standing time increased to 10 min. But after 10 min, as the time prolonged, the extraction efficiency decreased instead. It may be interpreted as that the interaction between the phthalates and C18-functionalized $Fe_3O_4@mSiO_2$ microspheres was strong, and the distribution equilibrium was easy to be achieved in only 10 min, but the analytes
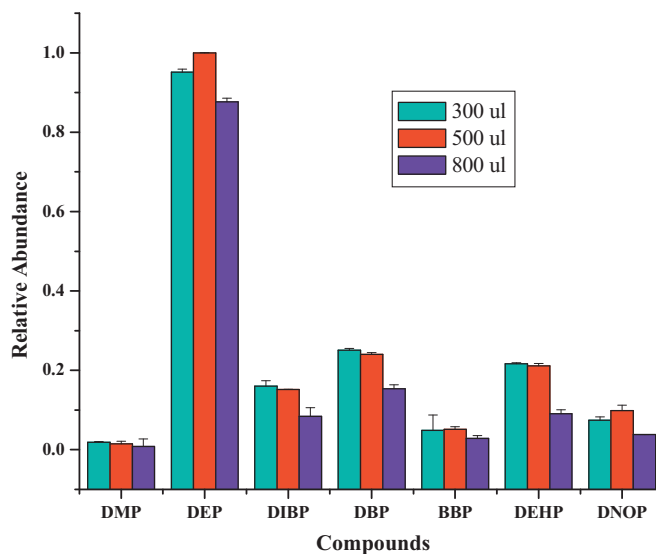

Fig. 7. The effect of volume of eluting solvent (300, 500 and 800 mL). Error bar represents disperse of 3 runs.
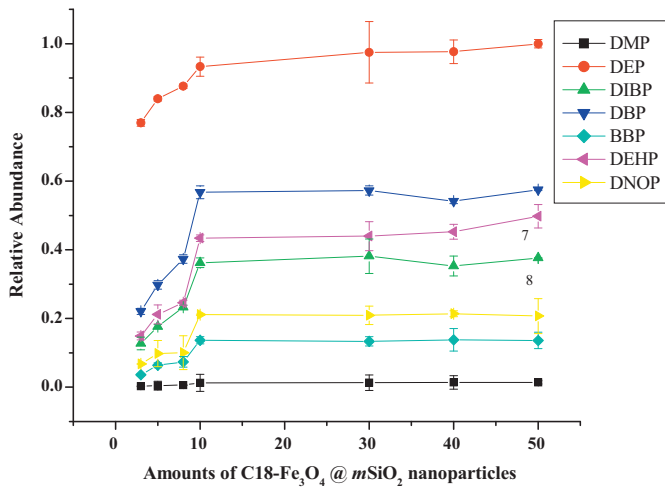
Fig. 8. The effect of amounts of C18–Fe$_3$O$_4$@mSiO$_2$ microspheres (3, 5, 8, 10, 20, 30, 40 and 50 mg). Error bar represents disperse of 3 runs.

could not be pulled down easily by the washing solvent with the further increase of time [43,44]. Hence, 10 min was selected as the best extraction time. Also, different eluting time (5, 10 and 15 min) was investigated. As shown in Fig. 10, 10 min was enough to receive the maximum extraction efficiency of all the analytes.

3.3. The investigation of anti-interference ability

Due to that hydrophobic extraction was performed in the interior pore (pore size, 4.1 nm) of magnetic mesoporous microspheres, and macromolecular proteins cannot enter into the mesoporous pore, the C18-functionalized magnetic mesoporous microspheres have the anti-interference ability to macromolecular proteins in the extraction process. Proteins, which are from rotten animal skins, fairs, metabolites, etc., widely exist in real water samples. These proteins in real water samples can affect the sample analysis results. In order to determine the anti-interference ability of the adsorbent to macromolecular proteins, BSA, which is a kind of macromolecular proteins, was used to determine whether the C18-functionalized Fe$_3$O$_4$@mSiO$_2$ microspheres could avoid being interfered by macromolecular proteins. As illustrated in Fig. 11, the
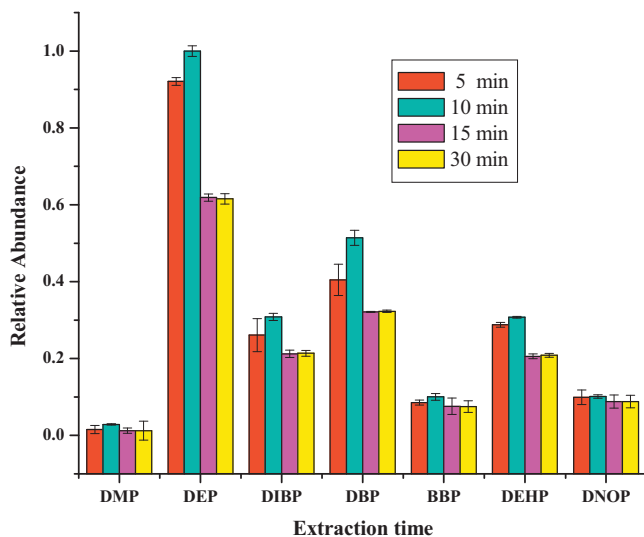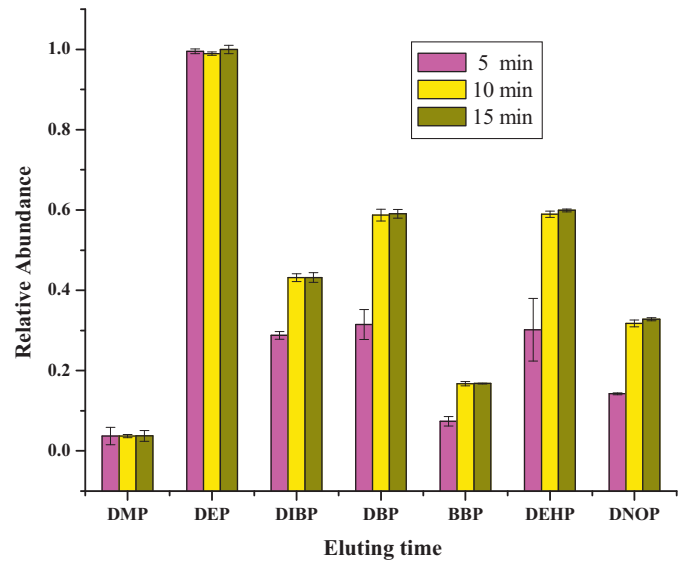

Fig. 10. The effect of different elution time (5, 10 and 15 min). Error bar represents disperse of 3 runs.

relative abundance of all target phthalates did not change obviously before and after adding BSA. The retention capacity of target compounds and BSA on this material was also investigated at 280 nm by UV spectrophotometry. After treating with the same condition, the absorbance values of bare material, the material extracting target compounds and the material extracting BSA were 2.79, 5.63 and 2.80, respectively. The results indicated that BSA was basically of no retention on the adsorbent. Therefore, the C18-functionalized Fe$_3$O$_4$@mSiO$_2$ adsorbent possesses high anti-interference capability because the narrow pore size distribution with 4.1 nm (Fig. 2) and could prevent the macromolecules from entering by size exclusion.

3.4. Validations of the method

The method validations such as linearity, repeatability, and limit of detection were studied. Good linearity was obtained and the corresponding values (R^2) were more than 0.991. Precision of the method varied from 4.8% to 11.2%. The LOD values were calculated

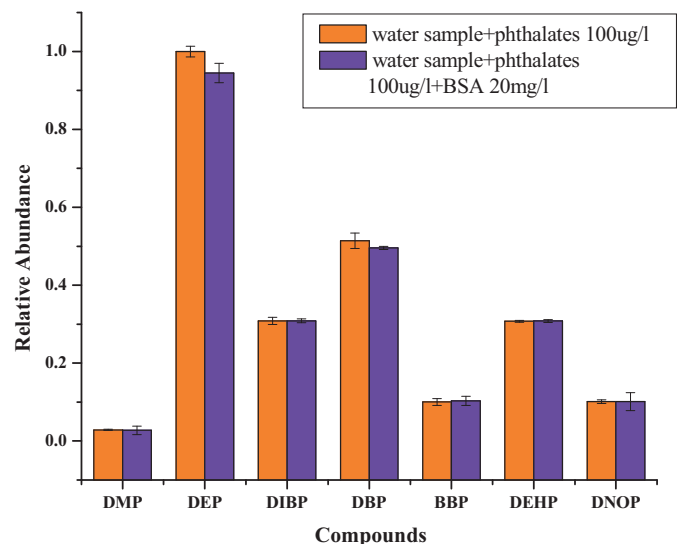**Fig. 9.** The effect of different extraction time (5, 10, 15 and 30 min). Error bar represents disperse of 3 runs.

Fig. 11. The examination of the anti-interference ability of the adsorbent to BSA. Error bar represents disperse of 3 runs.

Table 1
Validation for phthalates measured with C18-functionalied $Fe_3O_4@mSiO_2$ microspheres based on GC–MS method.

Compounds	Calibration curve	R^2	Linear range (μg/L)	RSD (%)	LOD (μg/L)	LOQ (μg/L)
DMP	$y = 22.922x - 585.58$	0.9958	50–3000	4.86	25	83
DEP	$y = 26.677x - 1144.9$	0.9971	50–3000	6.36	41	137
DIBP	$y = 25.113x - 1455.2$	0.9977	100–2000	7.08	60	200
DBP	$y = 33.2x - 1650.5$	0.9912	120–2000	10.0	77	256
BBP	$y = 5.7782x - 222.8$	0.9937	70–2500	11.2	46	153
DEHP	$y = 8.4254x + 399.49$	0.9911	115–2500	7.88	31	103
DNOP	$y = 7.7585x + 707.21$	0.9974	50–2500	5.11	37	123

on the basis of S/N = 3, and the values of all the analytes were from 25 to 77 μg/L. On the basis of S/N = 10, the LOQ values of the analytes were from 83 to 256 μg/L. All the results were shown in Table 1. The results showed that the proposed method based on magnetic micro solid-phase extraction technique was reliable.

3.5. Determination of phthalates in real water sample by the proposed method

Inspired by those satisfying enrichment results above, we further examined the feasibility of the C18-functionalized $Fe_3O_4@mSiO_2$ microspheres for the extraction of phthalates in real water. Under the optimal conditions, 10 mL real water sample from Yangpu River was extracted by 10 mg C18-functionalized $Fe_3O_4@mSiO_2$ microspheres with 10 min, and then eluted with 500 μL chloroform. Finally 1.0 μL of the eluent was injected into GC–MS. The total ion chromatogram of the real water sample was shown in Fig. 12. In the real water sample, DIBP, DBP, DEHP and BBP were detected. The calculated concentrations of the target phthalates were listed in Table 2. Due to that the C18-functionalized magnetic mesoporous silica microspheres have a very good magnetic responsivity, the analytes-adsorbed materials could be fast separated in 20 s by external magnetic field. This leads to that the whole analysis process required little time. Moreover, the C18-functionalized magnetic mesoporous silica microspheres have large surface area and high extraction efficiency. The results demonstrated that the proposed method based on C18-functionalized magnetic mesoporous silica microspheres could fast extract and analyze the phthalates in water sample.

Fig. 12. The chromatogram of tap water sample by the proposed method using selected ion monitoring (SIM) mode. The peaks marked with 1, 2, 3 and 4 represented the compounds of di-iso-butyl phthalate (DIBP), di-n-butyl phthalate (DBP), benzylbutyl phthalate (BBP) and di-(2-ethylhexyl) phthalate (DEHP), respectively.

Table 2
Concentrations of phthalates (μg/L) in real water sample.

Compounds	Water (mg/L)
Dimethyl phthalate (DMP)	ND
Diethyl phthalate (DEP)	ND
Di-iso-butyl phthalate (DIBP)	0.14
Di-n-butyl phthalate (DBP)	0.09
Benzylbutyl phthalate (BBP)	0.75
Di-(2-ethylhexyl) phthalate (DEHP)	0.08
Di-n-octyl phthalate (DNOP)	ND

ND: not detected.

4. Concluding remarks

In this work, novel C18-functionalized $Fe_3O_4@mSiO_2$ were synthesized through a facile one-pot sol–gel coating strategy and were successfully applied to the extraction and enrichment of phthalates in water samples. Thanks to the abundant exterior surface of silanol groups, the interior surface of functional C18 groups and the strong magnetic responsivity, the core–shell C18-functionalized $Fe_3O_4@mSiO_2$ microspheres display good dispersibility and fast magnetic response, which make the process of organic compounds extraction very simple, quick and efficient. More importantly, due to the strong hydrophobic–hydrophobic interaction between C18-functionalized $Fe_3O_4@mSiO_2$ microspheres and phthalates, the process of extraction and enrichment could be accomplished with a little amount of adsorbents in a short time of 10 min. Moreover, the C18-functionalized $Fe_3O_4@mSiO_2$ material could prevent the target analytes from being interfered by macromolecular proteins. From the experiment results, we can conclude that the proposed method based on C18-functionalized $Fe_3O_4@mSiO_2$ microspheres was fast and authentic, and could concentrate the target analytes selectively.

Acknowledgements

References

[1] H.H.P. Yiu, P.A. Wright, J. Mater. Chem. 15 (2005) 3690.
[2] F. Hoffmann, M. Cornelius, J. Morell, M. Froeba, Angew. Chem., Int. Ed. 45 (2006) 3216.
[3] A. Stein, B.J. Melde, R.C. Schroden, Adv. Mater. 12 (2000) 1403.
[4] A. Sayari, S. Hamoudi, Chem. Mater. 13 (2001) 3151.
[5] G.J. Soler-Illia, C. Sanchez, B. Lebeau, J. Patarin, Chem. Rev. 102 (2002) 4093.
[6] G. Kickelbick, Angew. Chem., Int. Ed. 43 (2004) 3102.
[7] R.J.P. Corriu, A. Mehdi, C. Reye, J. Mater. Chem. 15 (2005) 4285.
[8] B. Hatton, K. Landskron, W. Whitnall, D. Perovic, G.A. Ozin, Acc. Chem. Res. 38 (2005) 305.
[9] G.E. Fryxell, S.V. Mattigod, Y. Lin, H. Wu, S. Fiskum, K. Parker, F. Zheng, W. Yantasee, T.S. Zemanian, R.S. Addleman, J. Liu, K. Kemner, S. Kelly, X. Feng, J. Mater. Chem. 17 (2007) 2863.
[10] A. Walcarius, L. Mercier, J. Mater. Chem. 20 (2010) 4478.
[11] Y.H. Kim, B. Lee, K.H. Choo, S.J. Choi, Micropor. Mesopor. Mater. 138 (2011) 184.
[12] B. Lee, Y. Kim, H. Lee, J. Yi, Micropor. Mesopor. Mater. 50 (2001) 77.

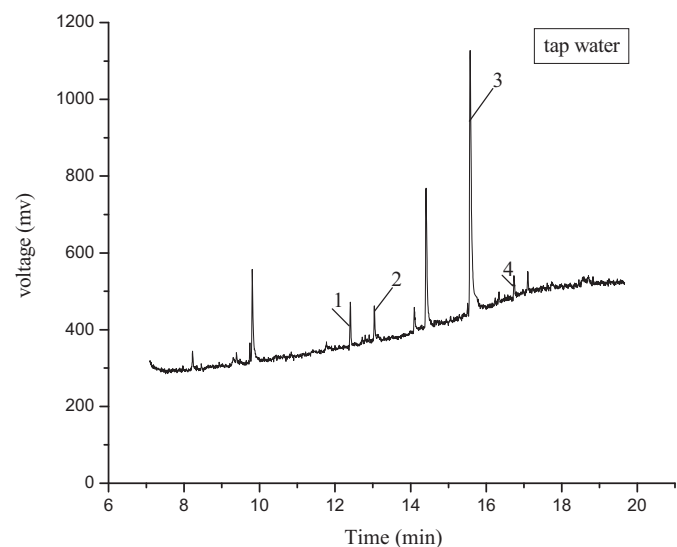[13] N. Baccile, F. Babonneau, Micropor. Mesopor. Mater. 110 (2008) 534.
[14] T. Shishido, T. Kawaguchi, T. Iwashige, K. Teramura, Y. Hitomi, T. Tanaka, Catal. Lett. 140 (2010) 121.
[15] J.H. Wang, S.R. Zheng, J.L. Liu, Z.Y. Xu, Chem. Eng. J. 165 (2010) 10.
[16] T. Sen, I.J. Bruce, T. Mercer, Chem. Commun. 46 (2010) 6807.
[17] X.C. Fu, X. Chen, J. Wang, J.H. Liu, X.J. Huang, Electrochim. Acta 56 (2010) 102.
[18] S. Rubio, D.P. Bendito, Trends Anal. Chem. 22 (2003) 470.
[19] H.Y. Niu, Y.Q. Cai, Y.L. Shi, F.S. Wei, S.F. Mou, G.B. Jiang, J. Chromatogr. A 1172 (2007) 113.
[20] N. Yao, H.M. Chen, H.Q. Lin, C.H. Deng, X.M. Zhang, J. Chromatogr. A 1185 (2008) 93.
[21] C.M.X. Zhang, H. Jiang, B.L. Tian, X.J. Wang, X.T. Zhang, Z.L. Du, Eng. Aspects 257 (2005) 521.
[22] X.L. Zhang, H.Y. Niu, S.X. Zhang, Y.Q. Cai, Anal. Bioanal. Chem. 397 (2010) 791.
[23] Q.S. Qu, S.W. Peng, D. Mangelings, X.Y. Hu, C. Yan, Electrophoresis 31 (2010) 556.
[24] H.Y. Niu, Y.Q. Cai, Anal. Chem. 81 (2009) 9913.
[25] Y.F. Sha, C.H. Deng, B.Z. Liu, J. Chromatogr. A 1198 (2008) 27.
[26] X.L. Zhang, H.Y. Niu, W.H. Li, Y.L. Shi, Y.Q. Cai, Chem. Commun. (2011), doi:10.1039/c1cc10300h.
[27] Y.H. Deng, D.W. Qi, C.H. Deng, X.M. Zhang, D.Y. Zhao, J. Am. Chem. Soc. 130 (2008) 28.
[28] H.M. Chen, S.S. Liu, H.L. Yang, Y. Mao, C.H. Deng, X.M. Zhang, P.Y. Yang, Proteomics 10 (2010) 930.
[29] X.H. Lu, H.Q. Liu, C.H. Deng, X.M. Yan, Chem. Commun. 47 (2011) 1210.
[30] S.S. Liu, H.M. Chen, X.H. Lu, C.H. Deng, X.M. Zhang, P.Y. Yang, Angew. Chem., Int. Ed. 49 (2010) 7557.
[31] A. Turner, M.C. Rawling, Mar. Chem. 68 (2000) 203.
[32] P. DiGennaro, E. Collina, A. Franzetti, M. Lasagni, A. Luridiana, D. Pitea, G. Bestetti, Environ. Sci. Technol. 39 (2005) 325.
[33] P.A. Clausen, V. Hansen, L. Gunnarsen, A. Afshari, P. Wolkoff, Environ. Sci. Technol. 38 (2004) 2531.
[34] S.D. Richardson, Anal. Chem. 78 (2006) 4021.
[35] H. Deng, X.L. Li, Q. Peng, X. Wang, J.P. Chen, Y.D. Li, Angew. Chem., Int. Ed. 44 (2005) 2782.
[36] K.L. Ding, B.J. Hu, G.M. An, R.T. Tao, H.Y. Zhang, Z.M. Liu, J. Mater. Chem. 19 (2009) 3725.
[37] W.R. Zhao, J.L. Gu, L.X. Zhang, H.R. Chen, J.L. Shi, J. Am. Chem. Soc. 127 (2005) 8916.
[38] L. Wang, J. Bao, L. Wang, F. Zhang, Chem. Eur. J. 12 (2006) 6341.
[39] B. Tan, S.E. Rankin, J. Phys. Chem. B 108 (2004) 20122.
[40] S.E. Rankin, A.P. Malanoski, F. van Swol, Mater. Res. Soc. Symp. Proc. 636 (2001) 121.
[41] S.B. Yoon, J.Y. Kim, J.H. Kim, Y.J. Park, K.R. Yoon, S.K. Park, J.S. Yu, J. Mater. Chem. 17 (2007) 1758.
[42] Z.Y. Ma, Y.P. Guan, H.Z. Liu, J. Polym. Sci. Polym. Chem. 43 (2005) 3433.
[43] S.X. Zhang, H.Y. Niu, Z.J. Hu, Y.Q. Cai, Y.L. Shi, J. Chromatogr. A 1217 (2010) 4757.
[44] S. Shen, J.F. Ren, J. Chen, X.H. Lu, C.H. Deng, X.G. Jiang, J. Chromatogr. A (2011), doi:10.1016/j.chroma.2011.05.060.